PAPER • OPEN ACCESS

Direct AFM observation of individual micelles, tile decorations and tiling rules of a dodecagonal liquid quasicrystal

View the article online for updates and enhancements.

Related content

- Defect structures in Frank–Kasper type square–triangle tiling of multimodal cage-type mesoporous silicas
  Yasuhiro Sakamoto

- Two-dimensional dodecagonal quasilattices
  N Niizeki and H Mitani

- Observation of a dodecagonal oxide quasicrystal and its complex approximant in the SrTiO3-Pt(1 1 1) system
  Sebastian Schenk, Stefan Förster, Klaus Meinel et al.

Direct AFM observation of individual micelles, tile decorations and tiling rules of a dodecagonal liquid quasicrystal

Ruibin Zhang[1,2]**, Xiangbing Zeng**[2] **and Goran Ungar**[1,2]

[1] Department of Physics, Zhejiang Sci-Tech University, Hangzhou 310018, People's Republic of China
[2] Department of Materials Science and Engineering, University of Sheffield, Sheffield S1 3JD, United Kingdom

E-mail: x.zeng@shef.ac.uk

Abstract

We performed an atomic force microscopy study of the dendron-based dodecagonal quasicrystal, the material that had been reported in 2004 as the first soft quasicrystal. We succeeded in orienting the 12-fold axis perpendicular to the substrate, which allowed the imaging of the quasiperiodic *xy* plane. Thus for the first time we have been able to obtain direct real-space information not only on the arrangement of the tiles, but also on their 'decorations' by the individual spherical micelles or 'nanoatoms'. The high-resolution patterns recorded confirm the square-triangle tiling, but the abundance of different nodes corresponds closely to random tiling rather than to any inflation rule. The previously proposed model of three types of decorated tiles, two triangular and one square, has been confirmed; the basic Frank–Kasper mode of alternating dense-sparse-dense-sparse layer stacking along *z* is confirmed too, each of the four sublayers being 2 nm thick. The consecutive dense layers are seen to be rotated by 90°, as expected. The 2 nm steps on the surface correspond to one layer of spheres, nonetheless with a dense layer always remaining on top, which implies a layer slip underneath and possibly the existence of screw dislocations.

Keywords: liquid crystal, dendrimer, self-assembly, Frank–Kasper phase, thin film, atomic force microscopy, cubic phase

(Some figures may appear in colour only in the online journal)

Introduction

In 2004 the first liquid quasicrystal (LQC) was reported [1], two decades after Shechtman's Nobel-winning discovery of quasicrystals in metals [2]. The 'forbidden' dodecagonal symmetry of the LQC was revealed by the distinctive 12-fold symmetry of the single-crystal x-ray diffraction pattern. Five basis vectors are required to index each diffraction peak with five integers. The structure of the LQC is believed to be analogous to that of dodecagonal quasicrystals found in metal alloys.

While in metals quasicrystals form from atoms, in the original LQC the 'atoms' were replaced by 'micelles', soft spheres formed by self-assembly of tree-like molecules known as dendrons (figure 1(a)).

The dodecagonal quasicrystal is quasiperiodic only in the *x*-*y* plane, while being periodic along the *z*-axis. The commonly accepted model of it can be constructed from quasiperiodic tiling [3, 4] of a plane using squares and equilateral triangles. The 3D arrangement of the atoms or micelles is then, as a first approximation, specified as 'decorations' of the tiles, which describe how atoms or micelles are arranged in each tile. Taking account of such decorations, there are three different types of tile: one square and two triangular, as shown in figure 1(b). The resulting model of dodecagonal quasicrystal
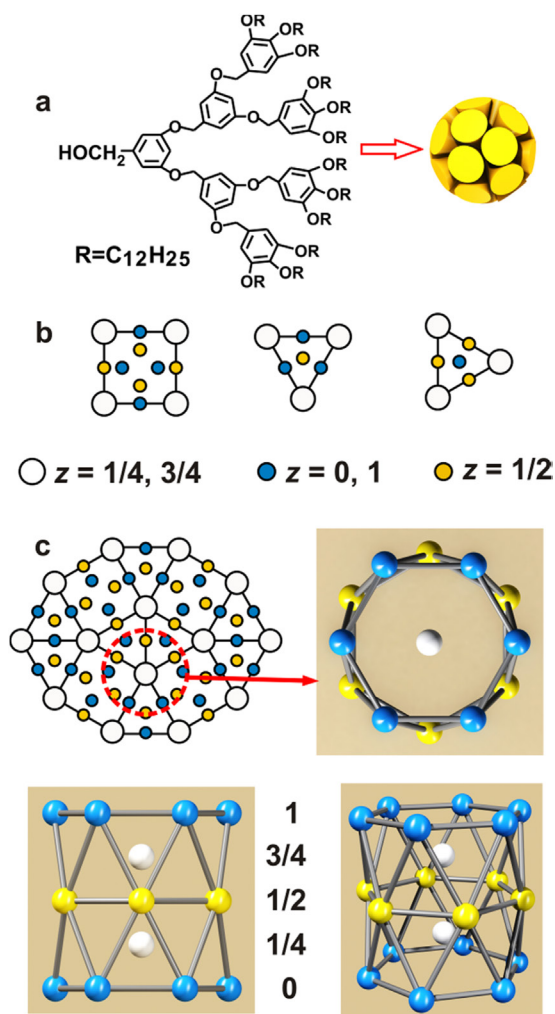
Figure 1. (a) Molecular structure of the dendron and schematic depiction of their self-assembly into a spherical micelle. (b) Three different decorated tiles viewed along the *z*-axis. The white dots represent micelles on the sparse layers at $z = 1/4$ and 3/4, while the blue and yellow dots indicate those on the dense layers at $z = 0$ and ½, respectively. (c) A decorated patch of the LQC. The 3D models show the hexagonal antiprisms whose centres are located at the corners of the square or triangular tiles.

Figure 2. AFM phase contrast images obtained from a dendron film where the 12-fold axis is parallel to the substrate. The ~8 nm periodicity along the 12-fold axis, and aperiodicity in the perpendicular direction, are clearly shown in (a). In the Fourier transform image (inset), the aperiodicity of the structure is indicated by the streaks along the perpendicular direction of intensity maxima. In (b), the alternating 'blue' and 'yellow' dense layers of micelles (see figure 1(c))—seen as white streaks—~4 nm apart.

contains alternating sparse and dense layers of spheres. These basic tiles are also found in two of the Frank–Kasper structures [5], with space group symmetry $Pm\overline{3}n$ (A15 phase) and $P4_2/mnm$ (σ-phase), respectively. These two FK phases have been observed in metal alloys [6] and in dendritic liquid crystals [7, 8], in the vicinity of the dodecagonal quasicrystal, i.e. they are both 'approximants' of the quasicrystal. Figure 1(c) shows a patch of the dodecagonal quasicrystal formed by micelles. Each micelle on a sparse layer is at the centre of a distorted hexagonal antiprism as marked by the red dashed circle.

With the discovery of the first LQC, research interest in quasicrystals has started to shift from metal alloys to other soft and hard materials with building blocks much larger than atoms. In addition to self-assembled spherical micelles from monodendrons [1, 9], columns and spheres formed from micro-phase segregation of block copolymers (BCPs)
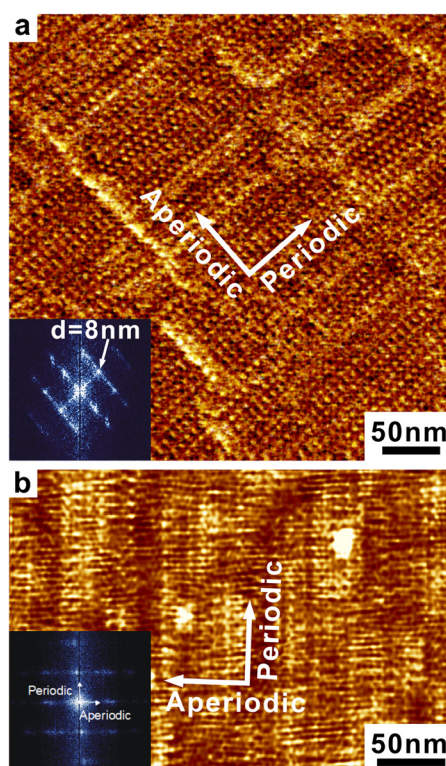
[10–12], nanoparticles [13], porous silica [14], and surfactants [15] have all recently been found to be able to form quasicrystalline structures. The majority of these show dodecagonal quasicrystalline symmetry.

For quasicrystals of metal alloys, the determination of atomic positions by microscopy is difficult due to limited resolution at the atomic scale. For LQC, on the other hand, the size of the spheres is of the order of nm and it is possible to determine the positions of individual micelles unambiguously. In this study we present the results of direct observation of an LQC by atomic force microscopy (AFM). It further proves the model presented in the previous study. The observed tiling pattern and defects in the dodecagonal LQC could provide valuable information about the nature of quasiperiodic order.

Experimental

The dendron used in this study is shown in figure 1(a). The synthesis is described in [1]. In order to prepare a thin film on a silicon surface from diluted solution without dewetting, the silicon wafer was treated with hexadecyltrichlorosilane (HTS) (from Fluorochem) vapor at 90 °C for 3 h. Dendron film of a
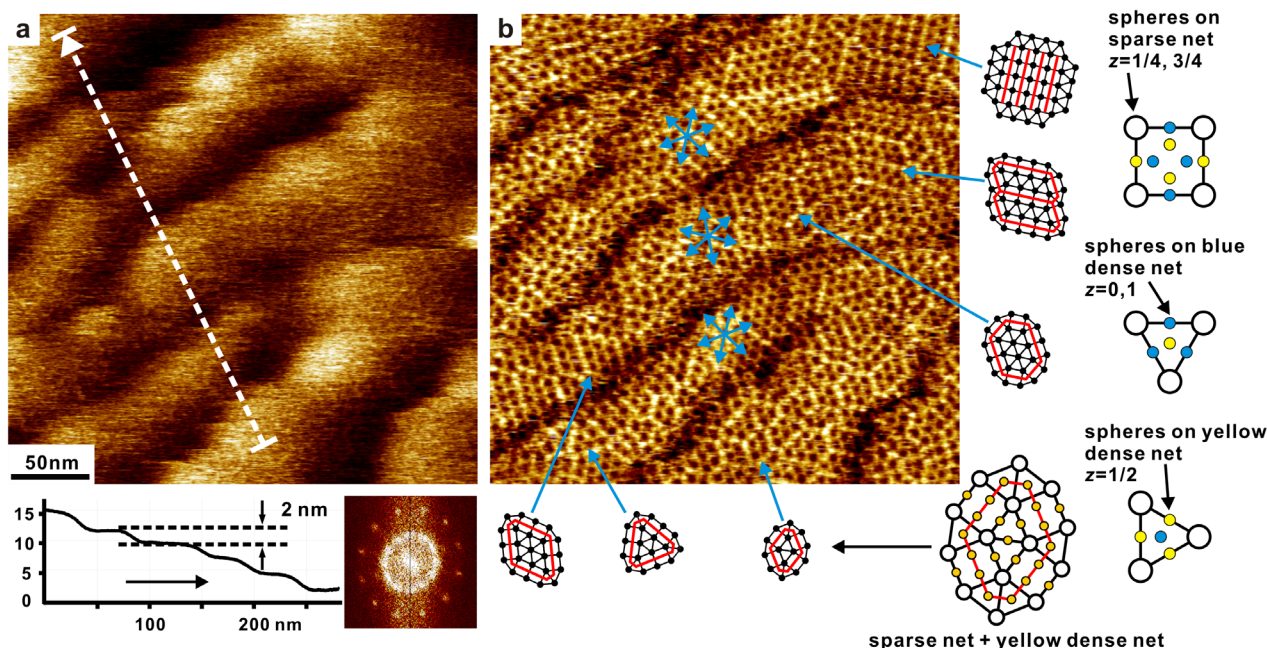
Figure 3. (a) AFM height image of the dodecagonal LQC obtained on the homeotropically aligned thin film. Bottom: the height scan through successive flat patches, showing steps of ~2 nm (note that a linear sloping background had been subtracted from the plot to compensate for layer tilt). The Fourier transformed pattern clearly shows 12-fold rotational symmetry. (b) Phase image showing the centres of the dodecagonal antiprisms as dark spots. Connecting these dark spots generates the square-triangle tiling of the plane. Some local tilings are shown at the side. Bright lines in (b) are formed by unresolved micelles in the top dense layer. The brightest lines run along the square tile bisectors, where the crowding is greatest; they are indicated by red lines in the schematic marginal tiling patterns. Note that the bright lines in (b) are aligned along three directions 60° apart from each other as indicated by the light blue arrow stars in the image. In neighbouring steps, the orientation of such lines is rotated by 90°, showing switching between blue and yellow top dense layers.

few μm thickness was cast from a 0.1 mg ml^{-1} toluene solution. The film was dried in a vacuum oven, followed by cooling from 90 °C to room temperature at 0.1 °C min^{-1}. Tapping mode AFM imaging was performed at room temperature on a Bruker Multimode 8 instrument with a Nanoscope V controller. An Asylum Cypher EF instrument was also used for some imaging at elevated temperature. All images shown below are recorded at room temperature where it was confirmed that the dodecagonal structure is stable for at least a year.

Results and discussion

The main obstacle to direct AFM observation of the LQC phase formed by dendron spheres is that the 12-fold axis prefers to lie parallel to the substrate surface (planar orientation). However, as shown in figure 2, certain features of the LQC phase are easily identified and are consistent with the general model. Thus, periodic stacking along the 12-fold axis and aperiodic stacking perpendicular to the 12-fold axis are easily identified. Additionally, the densely packed layers of micelles are clearly distinguished, and their periodicity of ~8 nm corresponds well to the 8.2 nm previously determined by x-ray diffraction [1]. However, more important information about tiling and tile decoration in the quasicrystalline plane is hard to retrieve from such images.

In this study we achieved homeotropic orientation (12-fold axis normal to the substrate surface) by preparing a thin film of only a few microns on alkylsilane-modified silicon surface.
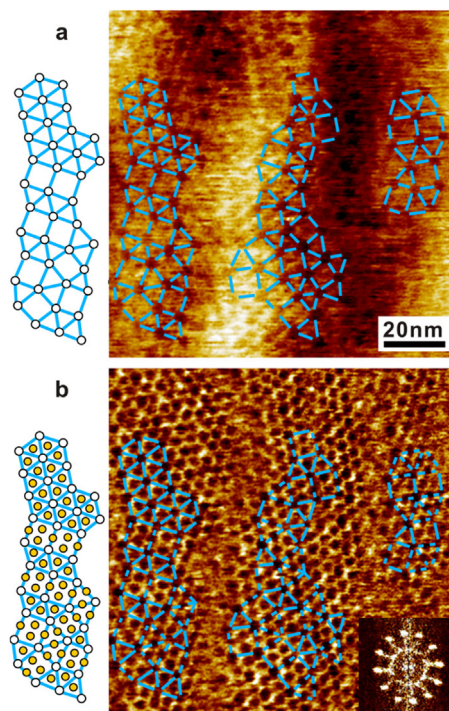

Figure 4. High resolution AFM image of homeotropically aligned dodecagonal LQC. (a) Height image. The dark spots are the centre of the antiprisms. (b) Corresponding phase image in which the dark spots are now individual micelles in the top dense layer ($z = 1$) and in the sparse layer immediately below it ($z = ¾$); they are marked by yellow and white dots, respectively, on the left. Inset: Fourier transformed pattern showing 12-fold symmetry. The overlaid blue networks are at the same position in (a) and (b).
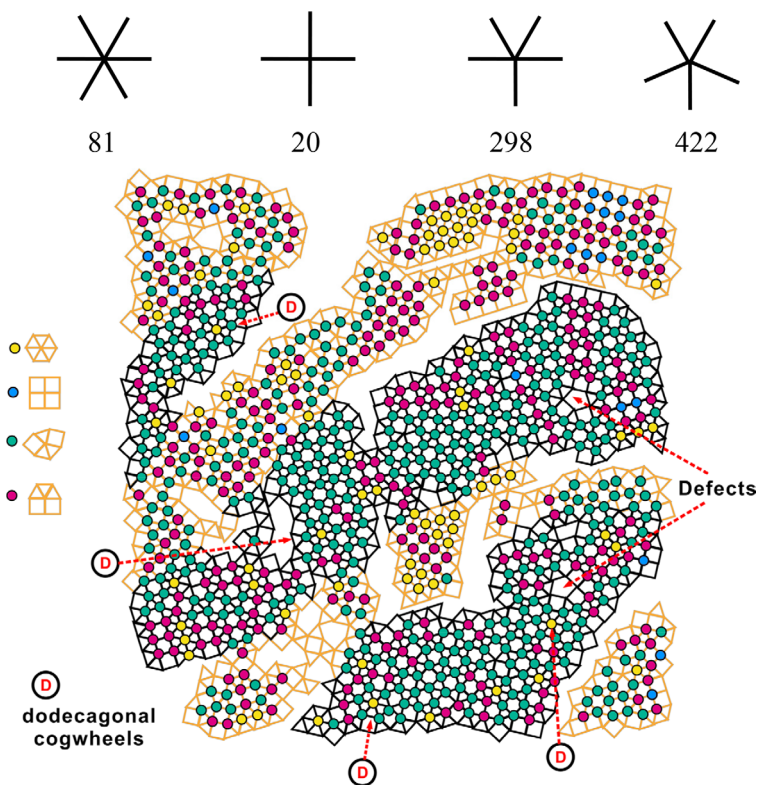
Figure 5. The tiling pattern of the LQC phase as observed in figure 3(b). Each node is coloured by the different arrangement of tiles around it. Yellow: 3^6; red: 4^4; green: $4.3.4.3^2$; magenta: $4^2.3^3$. Dodecagonal cogwheels and examples of dislocations are indicated as well.

Figure 3 shows an AFM phase image obtained on such a thin film using a tip of 10 nm radius. A 2D quasiperiodic network formed by dark spots can clearly be seen in the phase contrast image (figure 3(b)). The Fourier transformed pattern (inset, figure 3(a)) clearly shows 12-fold symmetry. The distance between these dark spots is measured as ~8 nm, which matches the size of the tile edge. The dark spots observed are not single dendron micelles but the centres of the antiprisms. According to the model in figure 1(c), the centre of the antiprism contains only one micelle on a sparse layer. Since the crowding is lower at the centre of a dense layer, it could be expected to generate less of a repulsive force on the probe and hence appear dark in the phase contrast image.

In figure 3 several flat patches are observed clearly, and the steps in height between neighbouring patches are ~2 nm (see height scan, bottom of figure 3(a)). This 2 nm step is only half of the expected 4 nm vertical distance between dense layers (between layers of blue and yellow micelles in figure 1(c)), and is discussed later. In each patch, the bright lines formed by outward protruding micelles align along three directions, 60° apart from each other (six-fold symmetry), and in neighbouring patches the orientation of such lines is rotated by 90°. Such behaviour is in fact expected from the model shown in figure 1(c), where blue and yellow micelles both line up along six directions mutually rotated by 60° within their own layer, but along different six directions, rotated by 90°, in adjacent layers.

A higher resolution height image (figure 4(a)) of the homeotropically aligned film also shows the centres of the antiprisms as dark spots. Connecting those nodes generates quasicrystal
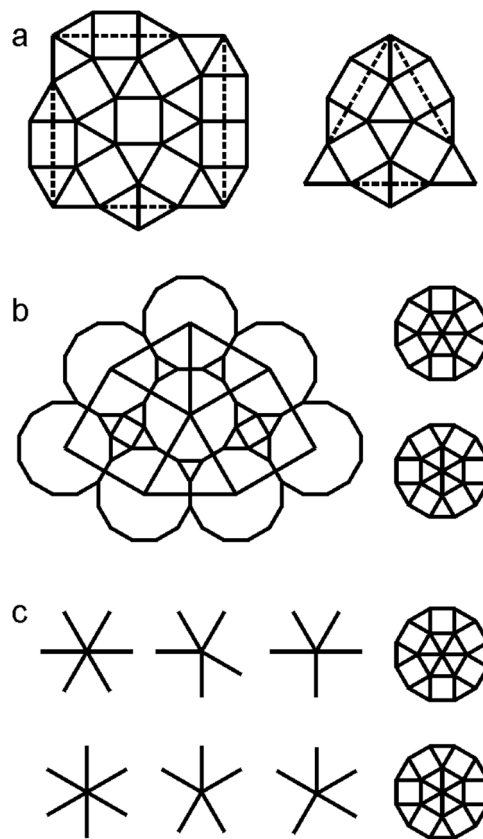

Figure 6. Inflation rules for the generation of dodecagonal quasiperiodic tilings. (a) Stampfli inflation rule. (b) Random Stampfli inflation rule. (c) Choice of dodecagon orientations in the extended Schlottmann rule.

Table 1. Different node types and their abundance in different tilings.

Node type ratios	$4.3.4.3^2$	$4^2.3^3$	4^4	3^6
Experimental	422	298	20	81
	51.4%	36.3%	2.4%	9.9%
Stampfli and Schlottmann	$23\sqrt{3} - 39$	$33 - 19\sqrt{3}$	0	$7 - 4\sqrt{3}$
	83.7%	9.1%	0%	7.2%
Simple random tiling $p = 0.3954$	$2p - 3p^2 + p^3$	$2p - 3p^2 + 2p^3 - p^4$	p^3	$(1-p)^4$
	38.4%	42.1%	6.2%	13.4%
$Pm\bar{3}n$	0	0	100%	0
$P4_2/mnm$	100%	0	0	0

tiling of squares and triangles (the overlaid blue nets). It can be seen more clearly in the copy of the left-hand net in the left margin, where the dark nodes are marked by white dots. The dark nodes are due to the centres of the antiprisms being lower than the periphery, which indicates that the top layer observed is the dense layer. In the corresponding phase image (figure 4(b)) individual micelles (dark dots) can be resolved on both the dense layer and the sparse layer below. This ability to detect the spheres in the lower (sparse) layer is due to the use of a very sharp tip in the recording of figure 4, capable of penetrating through the top face of the antiprism ($z = 1$) to the micelle on the sparse layer at $z = ¾$. The micelles on the sparse layer in the phase image, figure 4(b), can be identified at the same position as those dark spots observed in figure 4(a). The reason that both micelles at $z = 1$ and ¾ are seen in the phase but not in the height image is due to the sensitivity of the phase mode to the difference between the moduli of the harder aromatic core and the softer aliphatic corona of the micelles. It can be seen that the micelles decorate the tiles, both on the dense layers and the sparse layers, in exactly the same way as shown in the model in figure 1(b). This is the first unambiguous experimental proof of the tile decoration scheme of dodecagonal quasicrystals, either in metals or soft matter.

Another important question about dodecagonal quasicrystal is whether it is stabilized by energy or entropy. In the former case there should exist a ground state of square and triangular tilings which minimizes the system's energy, while in the latter the phase is based on random tiling, stabilized by the large number of different configurations of square-triangular tilings through phasonic flips [16]. Of course, whether there is such a clear cut division between the two situations is debatable, as both energy and entropy should contribute to the stability of the quasicrystalline phase.

For this reason we have constructed experimental square-triangle tiling (figure 5) by connecting the black spots in the phase image shown in figure 3(b). In the depicted patches there are 1175 triangles and 504 squares, the ratio being 2.33. This ratio is close to that of the square-triangle tilings generated according to the Stampfli inflation rule [3], as well as the extended Schlottmann rule [4] (as summarized in figure 6). In both cases, the ratio between the number of triangles and squares is $4/\sqrt{3} = 2.309$. It is interesting to note that this ratio is exactly the inverse of the ratio between the area of an equilateral triangle and a square of the same side length, suggesting a probable similar energy per unit area for square and triangular tiles. For comparison, in the $Pm\bar{3}n$ cubic phase
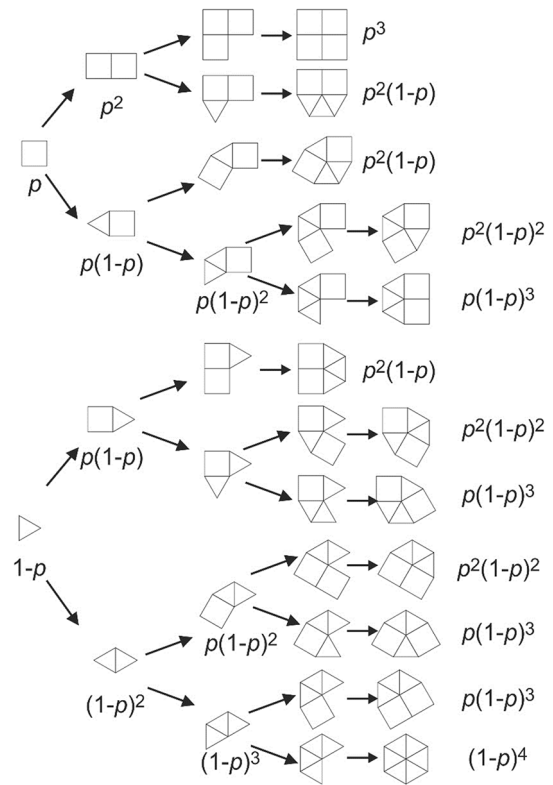

Figure 7. A simple random growth scheme of a vertex formation in dodecagonal tiling and for the estimation of the abundance of each node species. Around a vertex the tiles are added counter-clockwise. The probability of attaching a square to a growing vertex is p and that of a triangle is $(1 - p)$.

there are only squares and in the $P4_2/mnm$ tetragonal phase the ratio is 2.

However, a common feature of Stampfli and Schlottmann tilings is the abundance of dodecagonal cogwheels (figure 6). In contrast, only four such dodecagonal cogwheels can be found in the patches shown in figure 5. The ratios between different types of nodes in different tilings are listed in table 1. Among the four types of nodes possible for a square-triangle tiling, 4^4 is not allowed at all in the Stampfli and Schlottmann tilings but was observed experimentally, even though the percentage is low. The other key feature of our experimental observation is the abundance of nodes of type $4^2.3^3$—more than 1/3 of all nodes observed, i.e. much higher than in Stampfli and Schlottmann tilings. Overall the experimentally
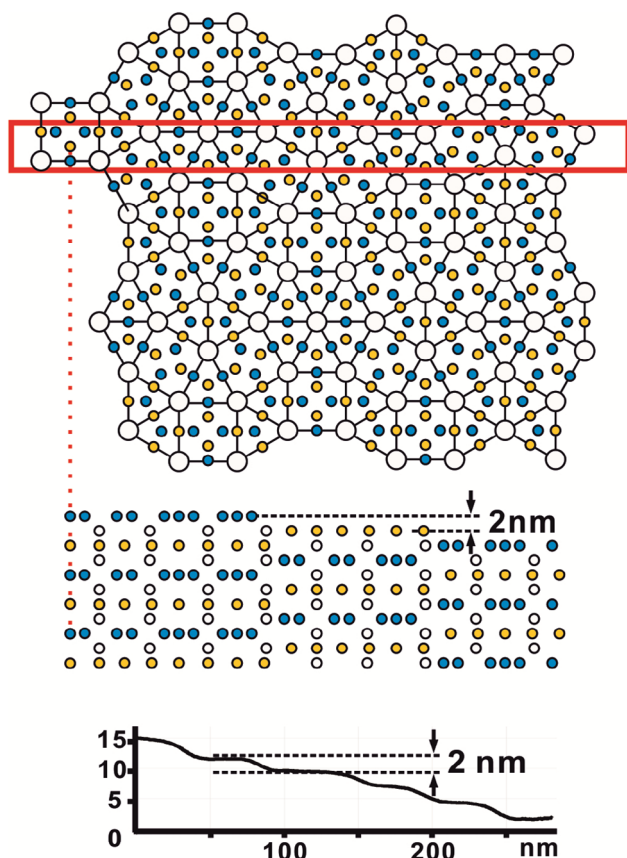
Figure 8. Possible explanation of the 2 nm steps observed between patches of dense layers.

observed patches are closer to a random square-triangular tiling than to those with stricter tiling rules.

For comparison, we have also examined a simple random square-triangle tiling growth scheme, where a vertex in the dodecagonal quasicrystal grows by statistically attaching a square or a triangle tile, with the probability being p (for squares) and $1 - p$ (for triangles) respectively. Ignoring the formation of dislocations and rearrangements of tiles during quasicrystal growth, the abundance of each node type can be estimated according to figure 7. The value of p is adjusted so that the numbers of triangles and squares have the desired ratio of $4/\sqrt{3}$. The results, as listed in table 1, indeed suggest that random tiling will result in a fraction of node type $4^2.3^3$ that is much higher than predicted by the above strict inflation rules. At the same time, the distribution of different node types in our random growth scheme is reasonably close to the experimental values, despite the crudeness of our estimation.

In addition to the randomness in the experimentally observed tiling pattern, it is also obvious from figure 5 that there are a relatively large number of dislocations, shown as mismatches between tiles present in the structure and patches that cannot be tiled with either squares or triangles. Some of the dislocation types bear a strong resemblance to those generated by a simulation carried out by Dotera *et al* [17].

Finally, as mentioned above, 2 nm steps were observed between patches of dense layers of micelles in AFM, while those expected from the model would be 4 nm, if continuity of dense and sparse layers was to be preserved. In order to explain this half-step, we propose that neighbouring patches are shifted vertically by 2 nm $= |\Delta z| = \frac{1}{4}$, or one layer of micelles, so that the dense layer of one patch is aligned with the sparse layer on the neighbouring patch (figure 8). In this way the top layer is always the dense layer, and the micelles in the sparse layers are never exposed to the surface. Moreover, we note that adjacent terraces appear as hexagonal lattices oriented 90° to each other (see the light-blue six arm stars in figure 3(b)); these form the upper and lower surface of the antiprisms. Thus as we move from top left to bottom right in figure 3 and go 'down the steps' of $\Delta z = -\frac{1}{4}$ in height, at the same time the underlying layers are shifting up by $\Delta z = +\frac{1}{4}$. Hence the orientations of the hexagonal nets on the top surface of the adjacent steps are rotated by 90°. The 2 nm vertical shift could be linked to the possible growth of the crystal around a screw location.

Conclusions

High-resolution AFM experiments were carried out to directly observe individual micelles and their packing in the dodocagonal liquid crystal of self-assembled spheres of dendron molecules. The results have confirmed the previously proposed tile decoration scheme of square and triangular tiles. Quasicrystal tiling is found to be close to random tiling of squares and triangles.

ORCID iDs

Xiangbing Zeng ⓘ https://orcid.org/0000-0003-4896-8080
Goran Ungar ⓘ https://orcid.org/0000-0002-9743-2656

References

[1] Zeng X B, Ungar G, Liu Y S, Percec V, Dulcey A E and Hobbs J K 2004 *Nature* **428** 157
[2] Shechtman D, Blech I, Gratias D and Cahn J W 1984 *Phys. Rev. Lett.* **53** 1951
[3] Stampfli P 1986 *Helv. Phys. Acta* **59** 1260
[4] Baake M, Klitzing R and Schlottmann M 1992 *Physica* A **191** 554
[5] Ungar G and Zeng X B 2005 *Soft Matter* **1** 95
[6] Gähler F 1988 *Quasicrystalline Materials* ed C Janot and J M Dubois (Singapore: World Scientific) p 272

[7] Balagurusamy V S K, Ungar G, Percec V and Johansson G 1997 *J. Am. Chem. Soc.* **119** 1539

[8] Ungar G, Liu Y S, Zeng X B, Percec V and Cho W D 2003 *Science* **299** 1208

[9] Ungar G, Percec V, Zeng X B and Leowanawat P 2011 *Isr. J. Chem.* **51** 1206

[10] Hayashida K, Dotera T, Takano A and Matsushita Y 2007 *Phys. Rev. Lett.* **98** 195502

[11] Zhang J and Bates F S 2012 *J. Am. Chem. Soc.* **134** 7636

[12] Gillard T M, Lee S W and Bates F S 2016 *Proc. Natl Acad. Sci. USA* **113** 5167

[13] Talapin D V, Shevchenko E V, Bodnarchuk M I, Ye X, Chen J and Murray C B 2009 *Nature* **461** 964

[14] Xiao C, Fujita N, Miyasaka K, Sakamoto Y and Terasaki O 2012 *Nature* **487** 349

[15] Yue K *et al* 2016 *Proc. Natl Acad. Sci. USA* **113** 14195

[16] Oxborrow M and Henley C L 1993 *Phys. Rev.* B **48** 6966

[17] Dotera T, Oshire T and Ziherl P 2014 *Nature* **506** 208